

RESEARCH ARTICLE

Placental malperfusion in response to intrauterine inflammation and its connection to fetal sequelae

Solange N. Eloundou¹, JiYeon Lee¹, Dan Wu², Jun Lei¹, Mia C. Feller^{1,3}, Maide Ozen^{1,3}, Yan Zhu¹, Misun Hwang², Bei Jia¹, Han Xie¹, Julia L. Clemens¹, Michael W. McLane¹, Samar AlSaggaf⁴, Nita Nair¹, Marsha Wills-Karp⁵, Xiaobin Wang⁶, Ernest M. Graham¹, Ahmet Baschat⁷, Irina Burd^{1*}

1 Integrated Research Center for Fetal Medicine, Division of Maternal Fetal Medicine, Department of Gynecology and Obstetrics, Johns Hopkins University, School of Medicine, Baltimore, MD, United States of America, **2** The Russell H. Morgan Department of Radiology and Radiological Science, Johns Hopkins University, School of Medicine, Baltimore, MD, United States of America, **3** Division of Neonatology, Department of Pediatrics, Johns Hopkins University, School of Medicine, Baltimore, MD, United States of America, **4** Department of Pathology, King Abdulaziz University, Jeddah, Kingdom of Saudi Arabia, **5** Department of Environmental Health and Engineering, Johns Hopkins University, School of Public Health, Baltimore, MD, United States of America, **6** Department of Population, Family and Reproductive Health, Center on Early Life Origins of Disease, Johns Hopkins University, School of Public Health, Baltimore, MD, United States of America, **7** Fetal Therapy, Department of Gynecology and Obstetrics, Johns Hopkins University, School of Medicine, Baltimore, MD, United States of America

* iburd@jhmi.edu



OPEN ACCESS

Citation: Eloundou SN, Lee J, Wu D, Lei J, Feller MC, Ozen M, et al. (2019) Placental malperfusion in response to intrauterine inflammation and its connection to fetal sequelae. PLoS ONE 14(4): e0214951. <https://doi.org/10.1371/journal.pone.0214951>

Editor: Leticia Reyes, University of Wisconsin - Madison, School of Veterinary Medicine, UNITED STATES

Received: November 21, 2018

Accepted: March 22, 2019

Published: April 3, 2019

Copyright: © 2019 Eloundou et al. This is an open access article distributed under the terms of the [Creative Commons Attribution License](https://creativecommons.org/licenses/by/4.0/), which permits unrestricted use, distribution, and reproduction in any medium, provided the original author and source are credited.

Data Availability Statement: All relevant data are within the manuscript and its Supporting Information files.

Funding: This work was supported by the Integrated Research Center for Fetal Medicine Fund, NICHDK08HD073315 (I.B.), and R21NS098018 (D.W.).

Competing interests: The authors have declared that no competing interests exist.

Abstract

Exposure to intrauterine inflammation (IUI) is associated with short- and long-term adverse perinatal outcomes. However, little data exist on utilizing placenta to prognosticate fetal injury in this scenario. Our study aimed to utilize imaging modalities to evaluate mechanisms contributing to placental injury following IUI exposure and correlated it to concomitant fetal brain injury. CD1 pregnant dams underwent laparotomies and received intrauterine injections of either lipopolysaccharide (LPS; a model of IUI) or phosphate-buffered saline (PBS). *In utero* ultrasound Doppler velocimetry of uterine and umbilical arteries and magnetic resonance imaging (MRI) of placental volumes with confirmatory immunohistochemical (vimentin) and histochemistry (fibrin) analyses were performed. ELISA for thrombosis markers, fibrinogen and fibrin was performed to analyze thrombi in placenta. Fetal brain immunohistochemistry was performed to detect microglial activation (ionized calcium-binding adaptor molecule 1, Iba1). On ultrasound, LPS group demonstrated elevated resistance indices, pulsatility indices and a greater occurrence of absent end-diastolic flow in the umbilical and uterine arteries. In the fetus, there was an increased cardiac Tei indices in the LPS group. MRI revealed decreased volume of placenta in the LPS group associated with placental thinning and placental endothelial damage on immunohistochemistry. Decreased fibrinogen content and more thrombi staining in placenta exposed to maternal LPS indicated the hypercoagulability. Furthermore, the expression of Iba1 was significantly associated with placental thickness ($r = -0.7890$, Pearson correlation coefficient). Our data indicate that IUI can trigger events leading to maternal placental malperfusion and fetal vessel resistance, as well as predispose the developing fetus to cardiac dysfunction and brain damage. Furthermore, our

data suggest that prenatal ultrasound can be a real-time clinical tool for assessing fetal risk for adverse neurologic outcomes following the potential IUI exposure.

Introduction

Intrauterine inflammation (IUI) during pregnancy is associated with numerous adverse perinatal outcomes initiated as part of the fetal inflammatory response syndrome (FIRS) [1,2,3]. FIRS contributes to fetal mortality, as well as a spectrum of short-term and long-term morbidities, including bronchopulmonary dysplasia and neurologic injury[3]. Of the approximately 6 million perinatal deaths each year, preterm birth associated with IUI may contribute to up to 27% of the mortality[4,5,6,7,8]. Timely diagnosis and prognostication of fetal injury may allow early intervention to prevent further sequelae of IUI exposure.

A major limitation of human studies is that placenta is obtained after delivery, thus there is a reduced ability to study placenta during pregnancy. Animal models overcome this limitation. Recently, researchers have demonstrated that ultrasound (US), with and without concomitant use of magnetic resonance imaging (MRI), may serve as a useful diagnostic tool for the detection of fetal neurological and placental complications during pregnancy [9,10]. However, placental imaging changes following IUI are not well-characterized, and whether these changes are correlated with fetal brain injury is not known.

In this study, we hypothesized that IUI results in hemodynamic and structural changes in placenta, which in turn lead to fetal sequelae. Specifically, we sought to determine whether placental changes occur as a result of thrombus formation and whether these changes are correlated with fetal microglial activation.

Materials and methods

Animal preparation

All care and treatment procedures were approved by the Animal Care and Use Committee of Johns Hopkins University (Hopkins-IACUC Protocol No. MO14M326) and were carried out in accordance with institutional standards. Pregnant CD-1 mice (Charles River Laboratories, Wilmington, MA, USA) were used for the study. On embryonic day 17 (E17), pregnant dams were subjected to a well-established model of IUI as per a previously described protocol [11,12,13,14]. Briefly, mice were placed under isoflurane anesthesia (Baxter # NDC 10019-360-60, Deerfield, IL, USA) before undergoing a mini-laparotomy; 25 μ g of lipopolysaccharide (LPS, Sigma Aldrich, St Louis, MO, USA from *E. coli* O55:B5, n = 56) in 100 μ l phosphate-buffered saline (PBS) or vehicle (PBS, n = 43) were injected between the first and second embryos of the lower right uterine horn. Routine laparotomy closure was performed, and the dams recovered.

Doppler examination

Doppler examination was performed for the uterine artery (UtA), placental and fetal sides of the umbilical artery (UA), and fetal Myocardial Performance Index (MPI/Tei) six hours after LPS-exposure in the IUI group and PBS-exposure in the control group. Briefly, general anesthesia was induced by inhalation of 5% isoflurane and oxygen at 3 L/minute and maintained with 1.5% isoflurane and oxygen at 2 L/minute. Doppler waveforms of the UtA were obtained at the level where the main UtA branches from the internal iliac artery. The systolic/diastolic

(S/D) ratio, resistance index (RI), pulsatility index (PI) and the presence of early diastolic notch were evaluated in UtA. Doppler waveforms of the placental and fetal sides were obtained at the placental cord insertion sites and fetal abdominal cord insertion sites, respectively. RI, PI and the presence of absent end-diastolic flow (AEDF) were evaluated in the UA. S/D ratio was calculated as (peak systolic velocity/end-diastolic velocity). RI was calculated as [(peak systolic velocity–end-diastolic velocity)/peak systolic velocity]. PI was calculated as [(peak systolic velocity–end-diastolic velocity)/mean velocity]. To measure the Tei index, Tissue Doppler Imaging (TDI) of the mitral annulus was obtained from the apical four-chamber view. The Tei index was calculated as [(isovolumic contraction time + isovolumic relaxation time)/ejection time]. Doppler waveforms of umbilical arteries and Tei index was obtained from both sides of the uterus (1 to 2 fetuses on the right, 1 to 2 fetuses on the left). Doppler waveforms of uterine arteries were measured on the right and left side. The right and left Doppler waveforms were not different. All Doppler waveforms were taken at an angle as close as possible to 0°. Vevo 770 (VisualSonics, Toronto, Ontario, Canada) was utilized for the Doppler evaluation.

MRI imaging

In utero MRI was performed six hours after LPS exposure. Pregnant dams were anesthetized with 1% isoflurane, along with air and oxygen, at a 3:1 ratio via a vaporizer. A horizontal 11.7T MRI scanner (Bruker Biospin, Billerica, MA, USA), with a 72-mm diameter quadrature transmitter coil and an eight-channel phased array rat body coil, was utilized. The multislice T2-weighted images were acquired with a Rapid Acquisition with Relaxation Enhancement (RARE) sequence using the following imaging parameters: field-of-view (FOV) = 40 x 32 mm, encoding matrix = 320 x 256 giving to an in-plane resolution of 0.125 x 0.125 mm, 0.5 mm slice thickness and 60 slices, echo time (TE)/repetition time (TR) = 24/5000, eight echo trains, four signal averages, and scan time of 11 minutes. The placental volumes were obtained by manual delineation of the placenta based on the T2-weighted images.

Histochemistry and immunohistochemistry (IHC)

Six hours after injection, isolated whole fetal brains and placentas from another set of mice with IUI—not those imaged—were fixed overnight at 4°C in 4% paraformaldehyde (PFA) (Affymetrix Inc., Cleveland, OH, USA). Tissue was then immersed in 30% sucrose (Sigma-Aldrich, St. Louis, MO, USA). Using Leica CM1950 cryostat (Leica Biosystems Inc., Buffalo Grove, IL, USA), the specimens were cut at 20 µm thickness and mounted on positively charged slides (Fischer Scientific). Fetal brains were cut coronally, and placentas were cut transversally. Two fetuses from the lower right horn and two fetuses from lower the left horn were sampled per each dam. Since the animals were treated in pregnancy, each dam represented an *n* of 1. The measurement of the placental thickness (total as well as maternal and fetal components) was done across the central cut surface of the placenta.

Routine hematoxylin and eosin (H&E) staining was performed on placentas to evaluate the morphological changes. For IHC, slides were incubated in PBS solution containing 0.05% Triton X-100 (Sigma-Aldrich) and 5% normal goat serum (Invitrogen, Carlsbad, CA, USA) for 30 minutes. Placental tissues were incubated with endothelial markers, rabbit anti-vimentin antibody (1:200, Abcam, Cambridge, MA, USA) and rat anti-CD31 (1:200, Abcam). Ionized calcium-binding adaptor molecule 1 (Iba1) is a marker of fetal brain injury [15]. Fetal brains were incubated with Iba1 antibody (1:400, Wako Chemicals, Richmond, VA, USA) [16]. To specify Iba1 staining, Ig G negative control was used in place of a primary rabbit antibody. Donkey anti-rabbit Alexa Fluor 568 and donkey anti-rat Alexa Fluor 488 fluorescent secondary antibodies were utilized (1:500, Life Technologies, Grand Island, NY, USA) along with

DAPI counter-staining. All images analyzed were obtained from Zeiss AxionPlan 2 Microscope System (Jena, Germany). The images for placental thickness measurements were taken under 5x magnification. IHC images of vimentin, CD31 and Iba1 quantification were obtained under 20x magnification. Five area of fields were chosen per animal. Image J (v1.48, <http://imagej.nih.gov/ij/>, National Institute of Health, Bethesda, MD, USA) was applied to measure the length of placenta using a straight line tool. The area measurements were performed using a threshold-based method. Placental data were obtained at the middle level. Fetal brain data were collected from the cortical area, including the cortex plate, subplate, intermediate zone, and ventricular zone.

Fibrinogen and fibrin measurement

Fibrinogen levels can be used as an indirect measure for the consumption of clotting factors following thrombus formation. Fibrinogen and fibrin in placenta were measured using an enzyme-linked immunosorbent assay (ELISA) kit purchased commercially (Abcam, Cambridge, MA, USA). Following the manufacturer's protocol, the plates were read using the CLARIOstar system (BMG Labtech, Cary, NC, USA), and final data were normalized by protein concentration. Histochemical staining (rapid phosphotungstic acid hematoxylin, PTAH, Polyscience Inc, Warrington, PA, US) was applied to the placenta for fibrin staining, according to the manufacturer's protocol.

Statistical analyses

The US-based indices, MRI-based placental volumetric measurements, H&E-based placental thickness measurements, and fibrinogen/fibrin levels in the LPS and PBS groups were compared using two-tailed Student's t-tests with unequal variance. Vimentin and Iba1 positive expression were determined through quantitative analyses; specifically, the vascular density was obtained using positive area divided by total area, and means of the measures were compared using the Student's t-test. Placental thickness was correlated with microglial activation (Iba1 expression) using the Pearson correlation analysis (Graphpad Prism). The statistically significant differences were recognized as $p < 0.05$.

Results

Uterine and umbilical artery insufficiency in placentas and the left ventricle Tei index increased in fetuses exposed to IUI

PBS- and LPS-exposed groups exhibited significant differences in Doppler waveforms at the UtA and both the placental and fetal sides of the UA. Specifically in the UtA, the S/D ratio (2.24 ± 0.28 vs. 4.30 ± 3.68 , $p < 0.05$), RI (0.55 ± 0.05 vs. 0.65 ± 0.16 , $p < 0.01$), PI (0.76 ± 0.10 vs. 1.01 ± 0.38 , $p < 0.01$) and rate of early diastolic notch (0.0% vs. 26.5%, $p < 0.05$) were significantly higher in the LPS group compared to the PBS group. The RI (0.85 ± 0.08 vs. 0.92 ± 0.06 , $p < 0.01$), PI (1.49 ± 0.23 vs. 1.71 ± 0.19 , $p < 0.01$) and rate of AEDF (0.0% vs. 18.4%, $p < 0.05$) in the placental side of the UA, as well as the RI (0.86 ± 0.08 vs. 0.94 ± 0.06 , $p < 0.01$), PI (1.54 ± 0.23 vs. 1.77 ± 0.21 , $p < 0.01$) and rate of AEDF (0.0% vs. 23.7%, $p < 0.05$) in the fetal side of the UA, were significantly higher in the LPS group compared to the PBS group (Fig 1A–1G).

Tei indices were significantly increased in the LPS group compared to the PBS group (0.37 ± 0.12 vs. 0.52 ± 0.14 , $p < 0.01$). The rate of abnormal Tei indices (> 0.44) was higher in the LPS group compared to the PBS group (13.6% vs. 70.0%, $p < 0.01$) (Fig 1H–1J). Considering the significant difference in fetal heart rates between the two groups (143 ± 40 vs. 97 ± 50 ,

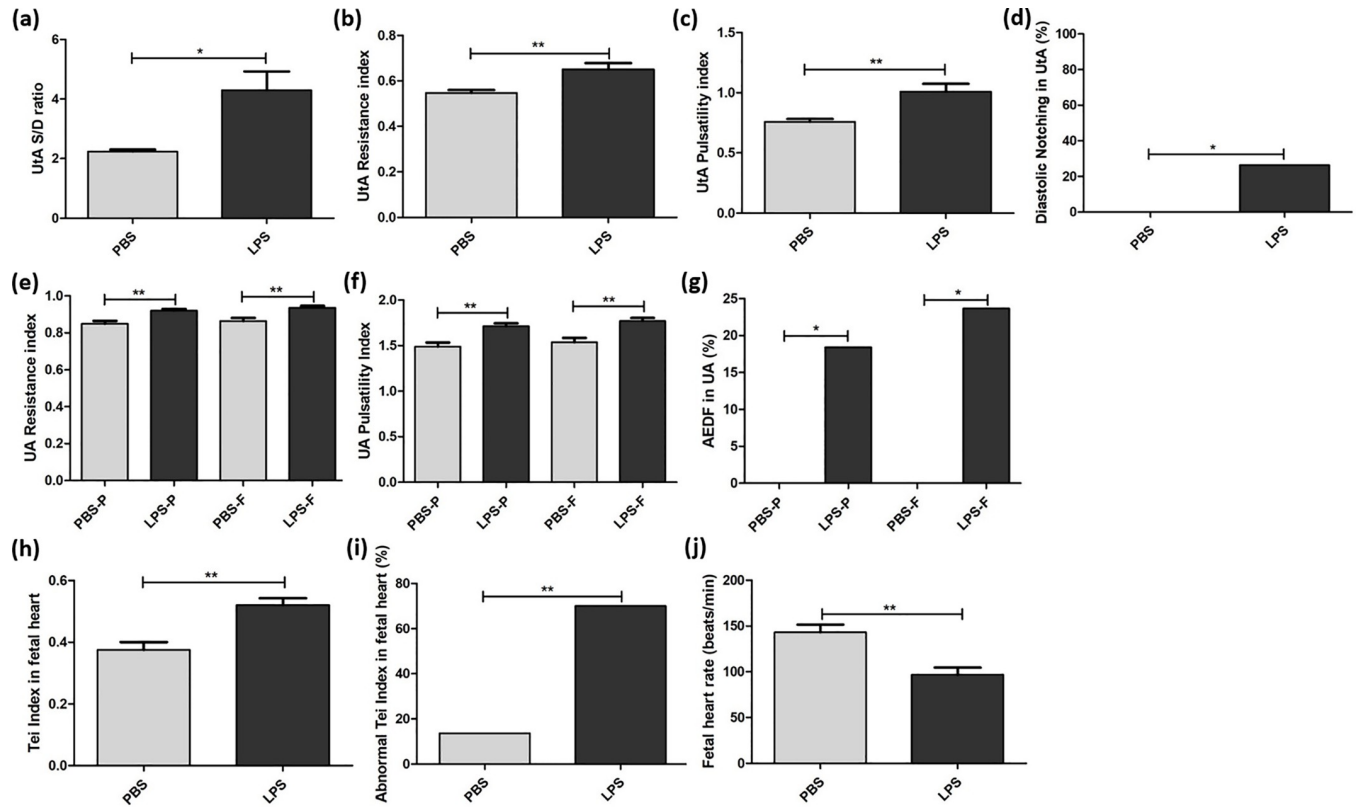


Fig 1. Uterine and umbilical artery insufficiency and abnormal Tei index of the fetal heart exposed to intrauterine inflammation. Doppler waveforms were interrogated six hours after phosphate-buffered saline (PBS) or lipopolysaccharide (LPS) exposure. Doppler was used to assess the uterine artery (UtA), placental side of the umbilical artery (UA) and fetal side of the UA in the PBS group, as well as the UtA, placental side of the UA and fetal side of the UA in the LPS group. (a) The systolic/diastolic (S/D) ratio, (b) resistance indices, (c) pulsatility indices and (d) rate of early diastolic notch in UtA were determined for the LPS group (n = 17 dams, 34 arteries) and the PBS group (n = 8 dams, 16 arteries). (e) Resistance indices, (f) pulsatility indices and (g) the rate of absent end-diastolic flow (AEDF) were found for both the placental (-P) and fetal (-F) sides of the UA in the LPS group (n = 17 dams, 38 pups) and the PBS group (n = 8 dams, 26 pups). Time intervals of Tissue Doppler for evaluating Tei indices are shown for the PBS group and the LPS group. (h) Tei indices, (i) the rate of abnormal Tei index (>0.44) and (j) fetal heart rates were compared for the LPS group (n = 17 dams, 40 pups) and the PBS group (n = 8 dams, 22 pups). *p<0.05, **p<0.01.

<https://doi.org/10.1371/journal.pone.0214951.g001>

p<0.01), a multivariate analysis was performed. The rate of abnormal Tei indices was still higher in the LPS group than the PBS group (adjusted odds ratio 18.24, 95% CI 3.62–91.84).

Decreased volume and thickness of placentas exposed to IUI

The mean volume of LPS-exposed placentas was significantly smaller than that of controls with a 13% decrease (Fig 2A and 2B, 155.3 ± 4.808 vs. 134.4 ± 8.746, p<0.05, two-tailed Student’s t-test with unequal variances). Additionally, H&E staining showed significantly reduced thickness in the LPS-exposed placentas compared to the PBS-exposed ones (Fig 2C and 2D, 2630 ± 26.47 vs. 2296 ± 29.08, p<0.0001, two-tailed Student’s t-test with unequal variances), with placental thinning found in both maternal and fetal components of LPS-exposed placentas.

Decreased CD31 and vimentin in placentas exposed to IUI

IHC staining for CD31 [17] and vimentin [18], endothelial cell markers, demonstrated less CD31 and vimentin expression in both the maternal and fetal segments of LPS-exposed placentas (Fig 3B & S1 Fig). Quantitative measurements indicated that the positive CD31

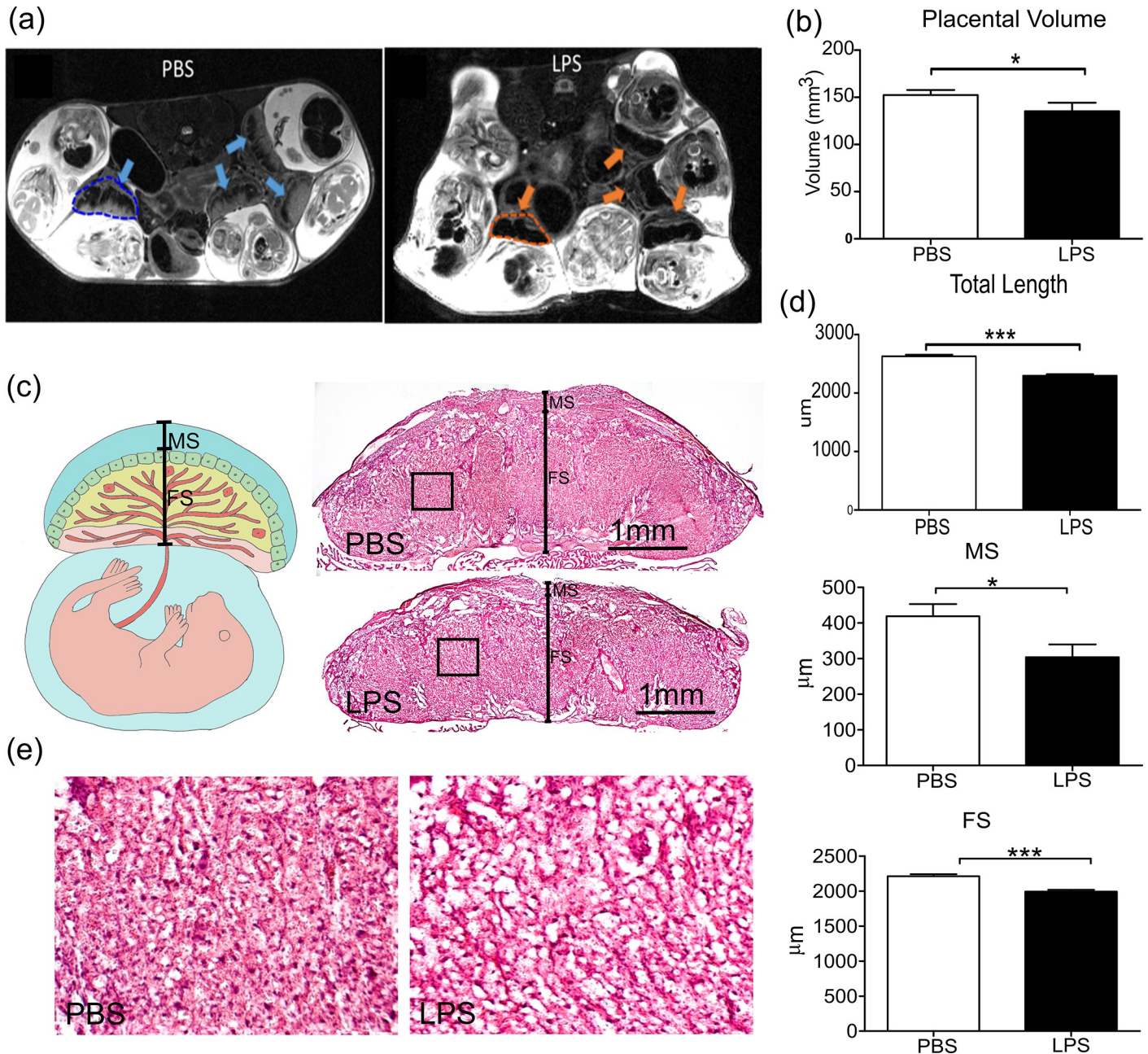


Fig 2. MRI imaging and analysis, revealing decreased volume and thickness of placentas exposed to intrauterine inflammation. (a) T2-weighted images of placentas in mice treated with phosphate-buffered saline (PBS) or lipopolysaccharide (LPS) were obtained. The blue and orange arrows note placental locations, while the dashed contours indicate examples of the manual delineation of the placentas (performed in 3D) for volumetric analysis. (b) 3D measurements shows the individual placenta volumes from the PBS (n = 15) and LPS (n = 14) groups. (c) Hematoxylin and eosin (H&E) stains were performed to compare LPS (n = 25) and PBS (n = 20) placental thicknesses at 5X magnification. The solid black line crossing the central cut surface of the placentas indicated the location of the measurements. The maternal segments (MS)–decidual zone–and fetal segments (FS) were identified as a compilation of junctional zone and labyrinth. (d) Statistical analysis shows the results of the H&E stain measuring maternal, fetal and total placental length at their thickest levels. (e) The images corresponded to the black boxes in (c) with high magnification. *p<0.05; ***p<0.001.

<https://doi.org/10.1371/journal.pone.0214951.g002>

(20.74 ± 0.64 vs. 16.38 ± 0.97) and vimentin (18.43 ± 0.62 vs. 14.58 ± 0.84) expression areas in the LPS group were significantly lower than that in the PBS group (Fig 3C, p<0.01, two-tailed Student's t-test).

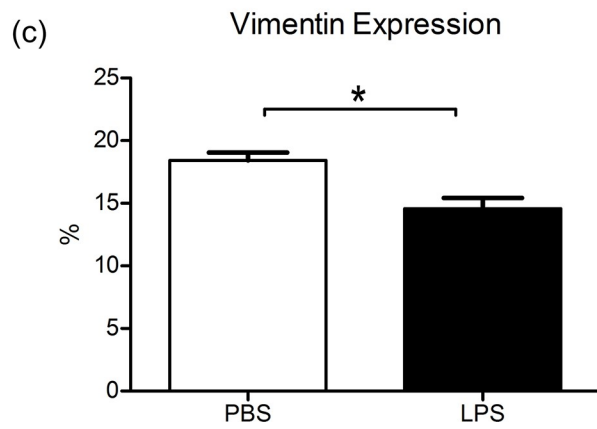
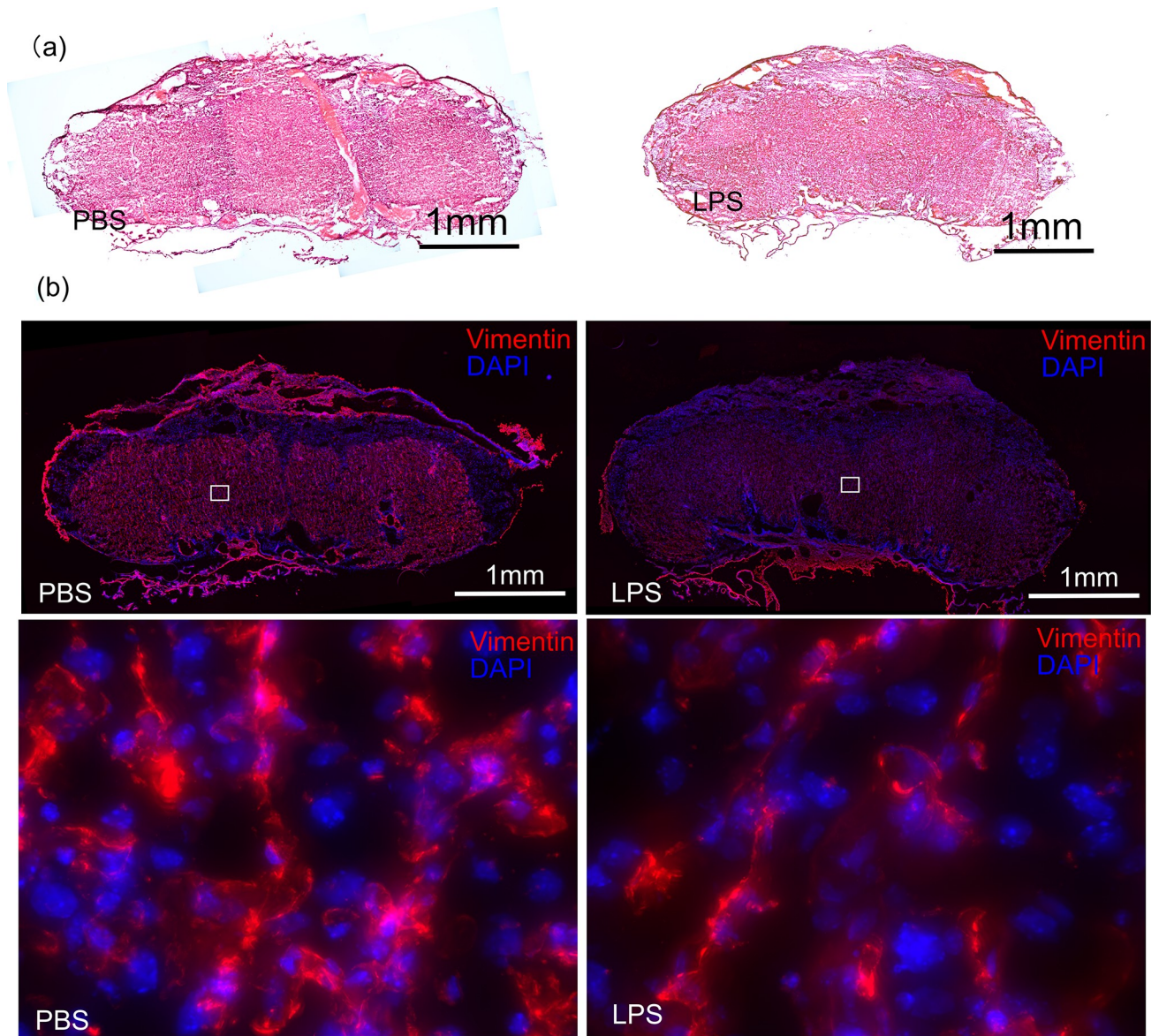


Fig 3. Vimentin staining of placentas, indicating the endothelial cells. (a) Hematoxylin and eosin (H&E) stains the neighbor sections indicates the central cut surface of the placentas. (b) Immunohistochemistry staining of vimentin (red) was shown for placentas exposed to phosphate-buffered saline (PBS, n = 5) or lipopolysaccharide (LPS, n = 5). DAPI (blue) stands for counter-staining of nuclei. The bottom panel is the magnification of the inserts in top panel. (c) Quantitative measurements show the percentage of vimentin expression in PBS and LPS placentas. *p<0.05.

<https://doi.org/10.1371/journal.pone.0214951.g003>

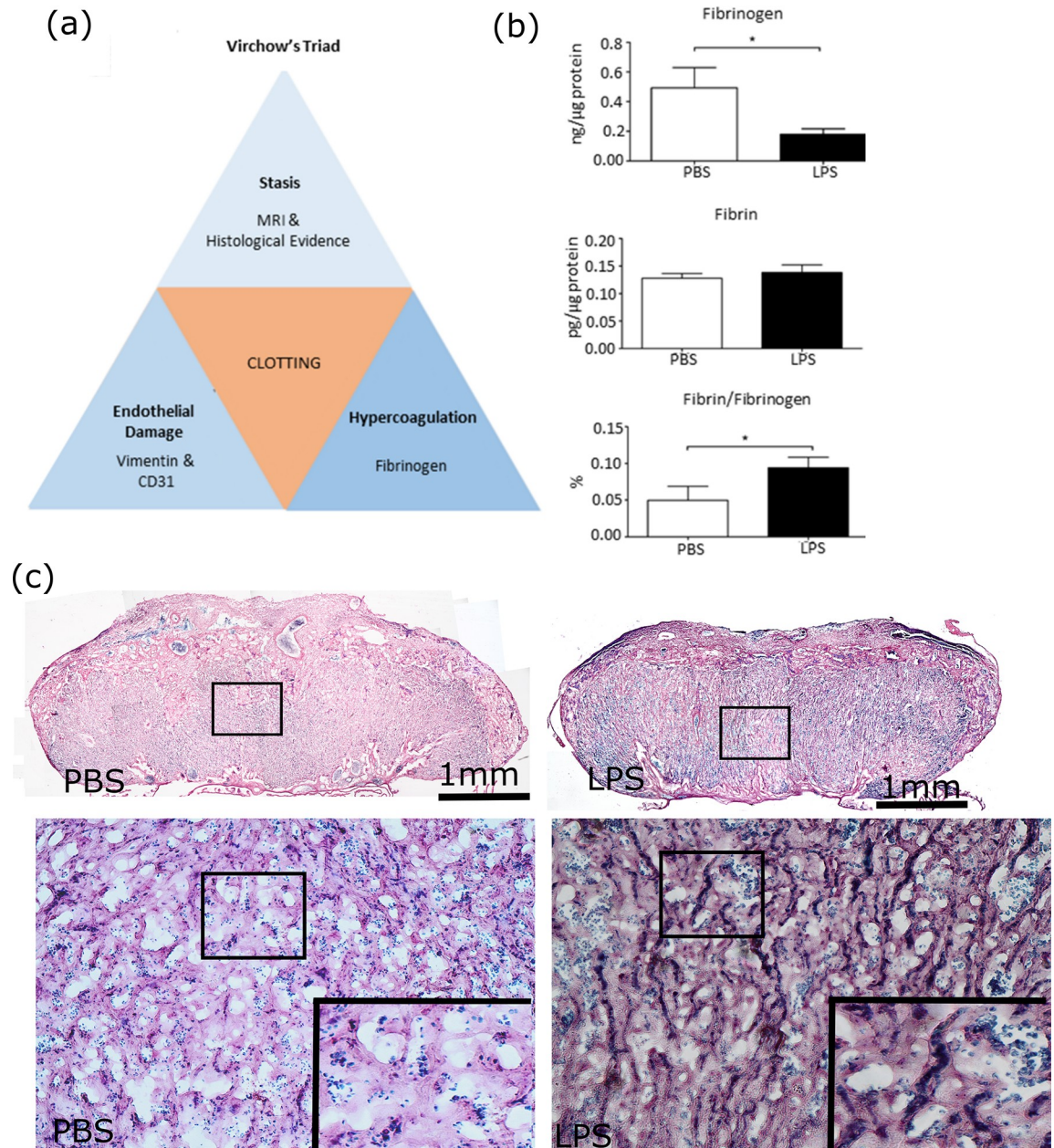


Fig 4. Virchow's Triad, including hypercoagulability suggested by decreased fibrinogen in placentas exposed to intrauterine inflammation. (a) This schematic illustrates the three primary factors that contribute to clot formation, according to Virchow's triad, as well as the lab techniques used to verify their presence in our study mice. (b) The graph shows the fibrinogen levels detected by enzyme-linked immunosorbent assay (ELISA) in placentas exposed to phosphate-buffered saline (PBS, n = 7) or lipopolysaccharide (LPS, n = 8). (c) Histochemical staining of placentas for fibrin show abundant fibrin-rich thrombi (dark blue) in the villi of placentas exposed to LPS. The inserts were the high magnification of the black box in the same panel. *p<0.05.

<https://doi.org/10.1371/journal.pone.0214951.g004>

Decreased fibrinogen in placentas exposed to IUI

ELISA with quantitative analysis revealed significantly less fibrinogen (0.1798 ± 0.03762 vs. 0.4931 ± 0.1370), comparable amounts of fibrin (0.1383 ± 0.0138 vs. 0.1278 ± 0.0087) and a significantly smaller percentage of fibrin to fibrinogen (0.0940 ± 0.0143 vs. 0.04980 ± 0.0189) in placentas exposed to IU LPS versus PBS (Fig 4B, $p < 0.05$, two-tailed Student's t-test). These results indicate a consumption of clotting factor with the formation of thrombi. Histochemical staining revealed fibrin-rich thrombi (dark blue) in some villi of placenta exposed to maternal LPS (Fig 4C).

Iba1 expression increased in brains of fetuses exposed to IUI

Images representative of Iba1 expression in the fetal brain following intrauterine exposure to LPS and PBS were selected (Fig 5A). Iba1 expression was significantly increased in fetal brains exposed to LPS as compared to PBS (Fig 5C, 0.6955 ± 0.0704 vs. 0.2171 ± 0.0333 , $p < 0.001$, Student's t-test). Additionally, placental thickness was negatively correlated to the percentage of microglial activation (Fig 5D, $p < 0.001$, $r = -0.7890$, Pearson correlation analysis).

Discussion

Utilizing a mouse model of IUI, for the first time, we evaluated if maternal and fetal malperfusion following exposure to IUI were associated with fetal sequelae (changes in cardiac Tei indices and fetal neuroinflammation). Consistent with other MRI studies [19,20], showing the association between the placental insufficiency and inflammatory pathway, our data demonstrate US-detectable hemodynamic changes in uterine and umbilical blood flow, which are confirmed by changes in placental volume and associated with endothelial damage and thrombi formation (decrease in fibrinogen). Most importantly, we demonstrate that placental thinning following IUI is associated with fetal microglial activation ($r = -0.7890$, Pearson correlation coefficient).

Virchow's triad asserts that hypercoagulability (as in pregnancy), injury to vasculature, and a disruption or interruption in blood flow collectively contribute to the development of thrombosis [21]. In our study, we demonstrate placental endothelial damage through vimentin and CD31 staining, as well as thrombosis through fibrinogen analysis. We speculate that the placental thinning, with concomitant damaged vasculature following IUI exposure may result in stagnant blood flow—the third component of Virchow's triad. Consequently, we propose that fetal microglial activation (a sign of fetal brain inflammation) may be associated with a placental thrombotic disruption in the passage of nutrients, gases, and toxins across the placenta and, hence, be a result of hypoxic-ischemic injury.

Studies have previously demonstrated that thrombi in the vasculature of the fetal side of the placenta were associated with severe injury to neonates, and the fetal brain seems particularly vulnerable to thrombotic disease based on its significant and constant receipt of circulating blood [22,23]. Specifically, Kraus and Acheen revealed that approximately one third of stillborns with extensive fetal thrombotic vasculopathy (FTV) in the placenta were also shown to suffer from thrombi in fetal organs, including the brain [23]. Moreover, the detection of thrombi in the fetal vasculature of the placenta has been linked to cerebral palsy in infants (18), whereas Lepais, Gaillot-Durand, Boutitie et al. observed a greater—though not significant—incidence of neurodevelopmental and language delays, as well as behavioral and motor disorders, in children whose placentas exhibited FTV lesions [24].

Maternal placental malperfusion is known to lead to abnormal uterine blood flow [25,26,27,28,29]. While malperfusion in the fetal compartment has the same effect on the umbilical waveform, fetuses exposed to such abnormalities are at risk for more widespread

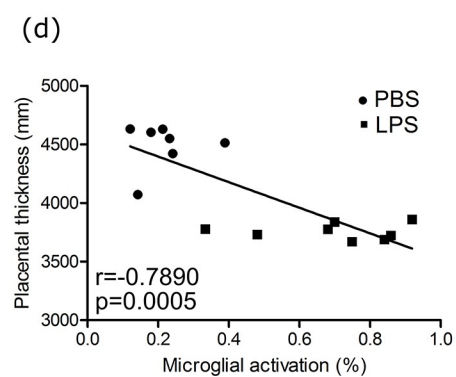
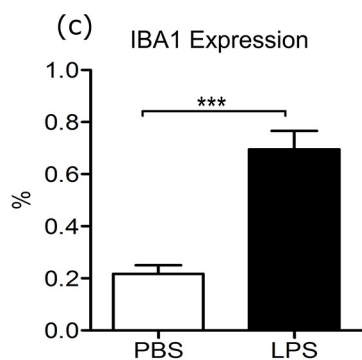
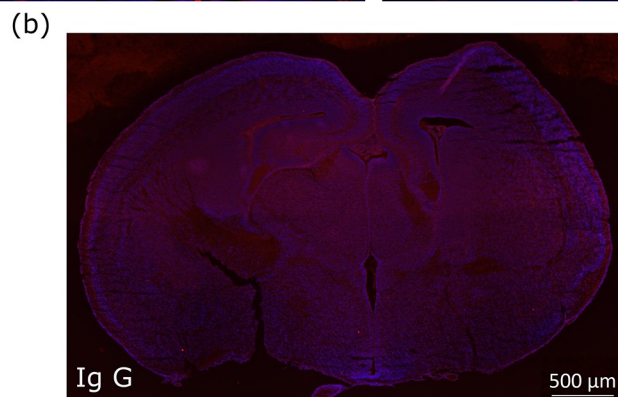
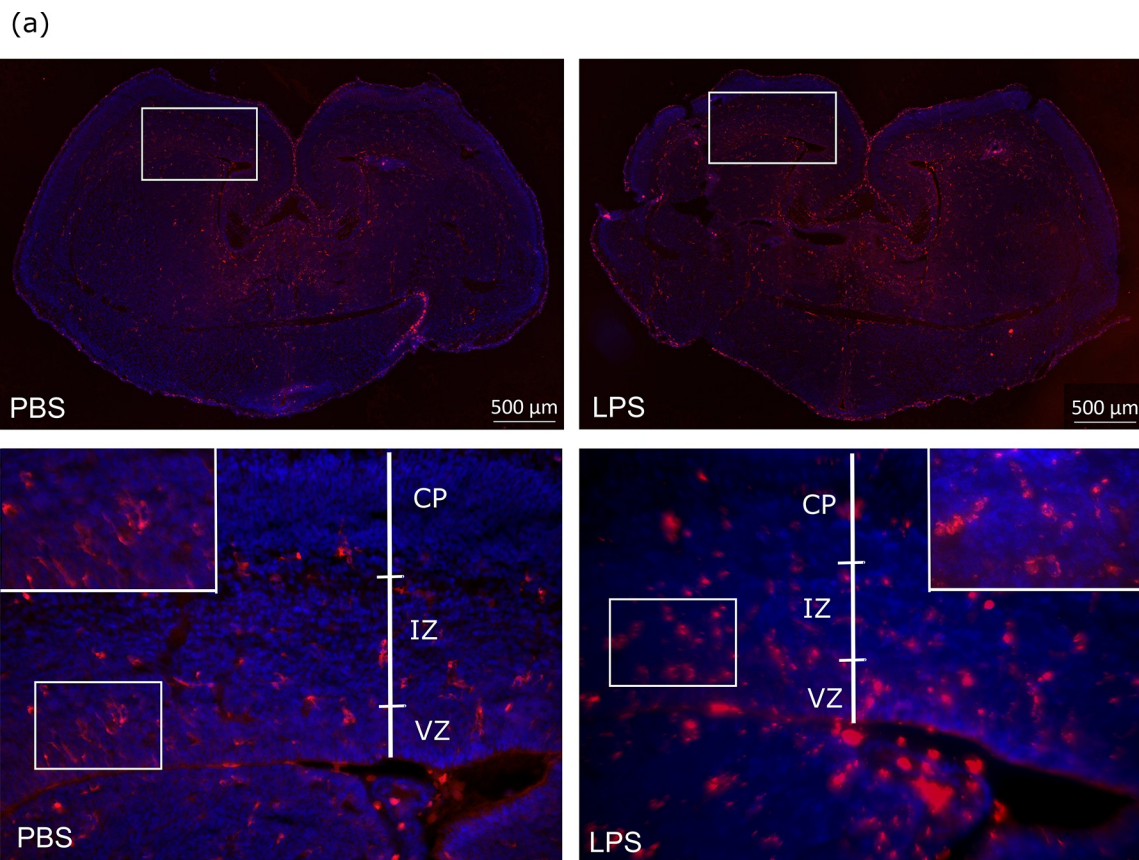


Fig 5. Iba 1 expression in fetal brain and correlation to placental thickness. (a) Representative images of ionized calcium-binding adaptor molecule 1 (Iba1) expression in fetal brain of E17 mice six hours after lipopolysaccharide (LPS) intra-uterine exposure are presented, the studied areas were the cortical area, including the cortex plate, intermediate zone, and ventricular zone. (b) Negative control image using rabbit Ig G in place of primary antibody. (c) Iba1 positive expression in fetal brains was determined through quantitative analysis as the percentage of Iba1 expression area within the image using Image J (PBS: n = 7, LPS: n = 8). (d) Placental thickness was correlated with microglial activation (Pearson correlation analysis). A Panel: blue represents DAPI stain for nuclei, and red represents Iba1 stain. *** p<0.001; scale bar: 50µm. CP: cortical plate, IZ: intermediate zone, VZ: ventricular zone.

<https://doi.org/10.1371/journal.pone.0214951.g005>

metabolic and cardiovascular sequelae, which have been linked to brain injury [30]. Furthermore, increased velocimetry indices are known to be concerning for fetal hypoxia and are associated with adverse perinatal outcomes, such as preeclampsia, preterm birth, fetal growth restriction (FGR), and increased cardiovascular and central nervous system problems in newborns [31,32,33,34,35]. Corollary to that, in our study, we demonstrate changes in Tei indices and fetal neuroinflammation following the observed changes in the fetoplacental hemodynamics.

The Tei index has mainly been used in amyloidosis, dilated cardiomyopathy, ischemic heart disease, and congestive heart failure; it is considered a useful predictor of global cardiac function, independent of both heart rate and blood pressure [36,37]. Some studies suggest that an increase in the Tei index may indicate ventricular dysfunction in fetuses with FGR, preeclampsia, and diabetes [38,39,40,41]. In clinical studies, the index has been used as an indicator of ventricular dysfunction in fetuses exposed to IUI [42]. Furthermore, fetuses suffering from FIRS who are unable to change cardiac compliance and exhibit worsening brain perfusion could develop fetal periventricular leukomalacia [43]. Taken together with our animal studies, the Tei index may be a useful predictor of fetal sequelae in cases suspicious for IUI exposure, such as preterm premature rupture of membranes (pPROM). Further clinical studies are needed to validate this tool. Furthermore, future research is needed to demonstrate whether heart dysfunction as a result of placental malperfusion may play a key role in the fetal neuroinflammation.

Although most prior studies examining UA Doppler indices have focused on placenta-based FGR, we speculate that this knowledge can be applied to identify patients at risk for developing sequelae of IUI. Our study is the first to document that IUI following intrauterine administration of LPS (mimicking the most common clinical scenario associated with preterm birth) leads to fetoplacental hemodynamic changes. Our study also highlights the potential importance of the level of interrogation of the UA along the umbilical cord where the sampling occurs.

Our study is supported by our prior work investigating MRI-based placental perfusion deficits following the exposure to IUI [44]. Specifically, we used MRI to examine placental damage following IUI and found a significant decrease in capillary blood volume and velocity, suggestive of vascular damage and blood flow disruption [44,45,46]. We speculate that these effects may contribute to the formation of a clot, subsequently decreasing placental volume. The results of our current study add further support to this speculation and correlate the acute placental injury following IUI to fetal sequelae [45].

Furthermore, our fetal MRI work previously demonstrated that fetal cortical injury could be detected from apparent diffusivity coefficient maps as early as six hours after exposure to inflammation and, in clinical studies, placental volumes are correlated with fetal brain volumes [44,46]. Taken together, US with or without concomitant MRI may serve as a useful clinical tool for delineating normal and pathological placentas, as well as predicting fetal sequelae in such cases of IUI exposure as preterm labor, pPROM, chorioamnionitis, FIRS, and potentially even thrombotic injuries.

In conclusion, our data provide evidence that IUI can trigger a sequence of events leading to acute maternal placental malperfusion and predispose the affected fetus to cardiac

dysfunction and brain inflammation. The combination of malperfusion and potential effects of placental thickness appear to be associated with fetal microglial activation. In this setting, further clinical investigations are necessary to establish the role of Doppler US as a clinical tool used to indirectly assess fetuses at risk for adverse neurologic outcomes following an exposure to IUI (e.g. preterm labor and pPROM).

Supporting information

S1 Fig. CD31 staining of placentas, indicating the endothelial cells. (a) Immunohistochemistry staining of CD31 (green) was shown for placentas exposed to phosphate-buffered saline (PBS, n = 5) or lipopolysaccharide (LPS, n = 5). DAPI (blue) stands for counter-staining of nuclei. (b) Quantitative measurements show the percentage of CD31 expression in PBS and LPS placentas. *p<0.05. (DOCX)

Acknowledgments

This work was supported by the Integrated Research Center for Fetal Medicine Fund, NICHDK08HD073315 (I.B.), and R21NS098018 (D.W.).

Author Contributions

Conceptualization: Irina Burd.

Data curation: Solange N. Eloundou, JiYeon Lee, Dan Wu, Jun Lei, Yan Zhu, Bei Jia, Han Xie, Julia L. Clemens, Michael W. McLane, Irina Burd.

Formal analysis: Solange N. Eloundou, JiYeon Lee, Dan Wu, Jun Lei, Yan Zhu, Bei Jia, Han Xie, Irina Burd.

Funding acquisition: Dan Wu, Irina Burd.

Investigation: Solange N. Eloundou, JiYeon Lee, Jun Lei, Misun Hwang, Irina Burd.

Methodology: JiYeon Lee, Dan Wu, Jun Lei, Michael W. McLane, Nita Nair, Irina Burd.

Project administration: Dan Wu, Mia C. Feller, Nita Nair, Irina Burd.

Resources: Dan Wu, Irina Burd.

Software: JiYeon Lee, Dan Wu, Irina Burd.

Supervision: Dan Wu, Maide Ozen, Samar AlSaggaf, Marsha Wills-Karp, Xiaobin Wang, Ernest M. Graham, Ahmet Baschat, Irina Burd.

Validation: JiYeon Lee, Dan Wu, Jun Lei, Irina Burd.

Visualization: Dan Wu, Jun Lei, Irina Burd.

Writing – original draft: Solange N. Eloundou, JiYeon Lee, Dan Wu, Jun Lei, Mia C. Feller, Maide Ozen, Julia L. Clemens, Irina Burd.

Writing – review & editing: JiYeon Lee, Jun Lei, Irina Burd.

References

1. Grether JK, Nelson KB (1997) Maternal infection and cerebral palsy in infants of normal birth weight. *JAMA* 278: 207–211. PMID: [9218666](https://pubmed.ncbi.nlm.nih.gov/9218666/)

2. Yoon BH, Romero R, Park JS, Kim CJ, Kim SH, et al. (2000) Fetal exposure to an intra-amniotic inflammation and the development of cerebral palsy at the age of three years. *Am J Obstet Gynecol* 182: 675–681. PMID: [10739529](https://pubmed.ncbi.nlm.nih.gov/10739529/)
3. Gotsch F, Romero R, Kusanovic JP, Mazaki-Tovi S, Pineles BL, et al. (2007) The fetal inflammatory response syndrome. *Clin Obstet Gynecol* 50: 652–683. <https://doi.org/10.1097/GRF.0b013e31811ebef6> PMID: [17762416](https://pubmed.ncbi.nlm.nih.gov/17762416/)
4. (2006) Neonatal and Perinatal Mortality. In: Organization WH, editor.
5. Goldenberg RL, Culhane JF, Iams JD, Romero R (2008) Epidemiology and causes of preterm birth. *Lancet* 371: 75–84. [https://doi.org/10.1016/S0140-6736\(08\)60074-4](https://doi.org/10.1016/S0140-6736(08)60074-4) PMID: [18177778](https://pubmed.ncbi.nlm.nih.gov/18177778/)
6. McCormick MC (1985) The contribution of low birth weight to infant mortality and childhood morbidity. *N Engl J Med* 312: 82–90. <https://doi.org/10.1056/NEJM198501103120204> PMID: [3880598](https://pubmed.ncbi.nlm.nih.gov/3880598/)
7. Goldenberg RL, Hauth JC, Andrews WW (2000) Intrauterine infection and preterm delivery. *N Engl J Med* 342: 1500–1507. <https://doi.org/10.1056/NEJM200005183422007> PMID: [10816189](https://pubmed.ncbi.nlm.nih.gov/10816189/)
8. Lettieri L, Vintzileos AM, Rodis JF, Albini SM, Salafia CM (1993) Does "idiopathic" preterm labor resulting in preterm birth exist? *Am J Obstet Gynecol* 168: 1480–1485. PMID: [8498431](https://pubmed.ncbi.nlm.nih.gov/8498431/)
9. Lax A, Prince MR, Mennitt KW, Schwebach JR, Budorick NE (2007) The value of specific MRI features in the evaluation of suspected placental invasion. *Magn Reson Imaging* 25: 87–93. <https://doi.org/10.1016/j.mri.2006.10.007> PMID: [17222719](https://pubmed.ncbi.nlm.nih.gov/17222719/)
10. Levine D, Barnes PD, Madsen JR, Li W, Edelman RR (1997) Fetal central nervous system anomalies: MR imaging augments sonographic diagnosis. *Radiology* 204: 635–642. <https://doi.org/10.1148/radiology.204.3.9280237> PMID: [9280237](https://pubmed.ncbi.nlm.nih.gov/9280237/)
11. Dada T, Rosenzweig JM, Al Shammary M, Firdaus W, Al Rebh S, et al. (2014) Mouse model of intra-uterine inflammation: sex-specific differences in long-term neurologic and immune sequelae. *Brain Behav Immun* 38: 142–150. <https://doi.org/10.1016/j.bbi.2014.01.014> PMID: [24486323](https://pubmed.ncbi.nlm.nih.gov/24486323/)
12. Leitner K, Al Shammary M, McLane M, Johnston MV, Elovitz MA, et al. (2014) IL-1 receptor blockade prevents fetal cortical brain injury but not preterm birth in a mouse model of inflammation-induced preterm birth and perinatal brain injury. *Am J Reprod Immunol* 71: 418–426. <https://doi.org/10.1111/aji.12216> PMID: [24592965](https://pubmed.ncbi.nlm.nih.gov/24592965/)
13. Lei J, Firdaus W, Rosenzweig JM, Alrebh S, Bakhshwin A, et al. (2015) Murine model: maternal administration of stem cells for prevention of prematurity. *Am J Obstet Gynecol* 212: 639 e631–610.
14. Breen K, Brown A, Burd I, Chai J, Friedman A, et al. (2012) TLR-4-dependent and -independent mechanisms of fetal brain injury in the setting of preterm birth. *Reprod Sci* 19: 839–850. <https://doi.org/10.1177/1933719112438439> PMID: [22825738](https://pubmed.ncbi.nlm.nih.gov/22825738/)
15. Kirik OV KD (2016) Brain Microglia and Microglial Markers. *Neurosci Behav Physiol* 46: 7.
16. Vermillion MS, Lei J, Shabi Y, Baxter VK, Crilly NP, et al. (2017) Intrauterine Zika virus infection of pregnant immunocompetent mice models transplacental transmission and adverse perinatal outcomes. *Nat Commun* 8: 14575. <https://doi.org/10.1038/ncomms14575> PMID: [28220786](https://pubmed.ncbi.nlm.nih.gov/28220786/)
17. Lertkiamongkol P, Liao D, Mei H, Hu Y, Newman PJ (2016) Endothelial functions of platelet/endothelial cell adhesion molecule-1 (CD31). *Curr Opin Hematol* 23: 253–259. <https://doi.org/10.1097/MOH.000000000000239> PMID: [27055047](https://pubmed.ncbi.nlm.nih.gov/27055047/)
18. Liu T, Guevara OE, Warburton RR, Hill NS, Gaestel M, et al. (2010) Regulation of vimentin intermediate filaments in endothelial cells by hypoxia. *Am J Physiol Cell Physiol* 299: C363–373. <https://doi.org/10.1152/ajpcell.00057.2010> PMID: [20427712](https://pubmed.ncbi.nlm.nih.gov/20427712/)
19. Girardi G, Fraser J, Lennen R, Vontell R, Jansen M, et al. (2015) Imaging of activated complement using ultrasmall superparamagnetic iron oxide particles (USPIO)—conjugated vectors: an in vivo in utero non-invasive method to predict placental insufficiency and abnormal fetal brain development. *Mol Psychiatry* 20: 1017–1026. <https://doi.org/10.1038/mp.2014.110> PMID: [25245499](https://pubmed.ncbi.nlm.nih.gov/25245499/)
20. Girard S, Tremblay L, Lepage M, Sebire G (2010) IL-1 receptor antagonist protects against placental and neurodevelopmental defects induced by maternal inflammation. *J Immunol* 184: 3997–4005. <https://doi.org/10.4049/jimmunol.0903349> PMID: [20181892](https://pubmed.ncbi.nlm.nih.gov/20181892/)
21. Stanifer JW (2016) Virchow's triad: Kussmaul, Quincke and von Recklinghausen. *J Med Biogr* 24: 89–100. <https://doi.org/10.1177/0967772013520101> PMID: [24658214](https://pubmed.ncbi.nlm.nih.gov/24658214/)
22. Kraus FT (1997) Cerebral palsy and thrombi in placental vessels of the fetus: insights from litigation. *Hum Pathol* 28: 246–248. PMID: [9023410](https://pubmed.ncbi.nlm.nih.gov/9023410/)
23. Kraus FT, Acheen VI (1999) Fetal thrombotic vasculopathy in the placenta: cerebral thrombi and infarcts, coagulopathies, and cerebral palsy. *Hum Pathol* 30: 759–769. PMID: [10414494](https://pubmed.ncbi.nlm.nih.gov/10414494/)
24. Lepais L, Gaillot-Durand L, Boutitie F, Lebreton F, Buffin R, et al. (2014) Fetal thrombotic vasculopathy is associated with thromboembolic events and adverse perinatal outcome but not with neurologic

- complications: a retrospective cohort study of 54 cases with a 3-year follow-up of children. *Placenta* 35: 611–617. <https://doi.org/10.1016/j.placenta.2014.04.012> PMID: 24862569
25. Dikshit S (2011) Fresh look at the Doppler changes in pregnancies with placental-based complications. *J Postgrad Med* 57: 138–140. <https://doi.org/10.4103/0022-3859.81880> PMID: 21654141
 26. Spinillo A, Gardella B, Bariselli S, Alfei A, Silini E, et al. (2012) Placental histopathological correlates of umbilical artery Doppler velocimetry in pregnancies complicated by fetal growth restriction. *Prenat Diagn* 32: 1263–1272. <https://doi.org/10.1002/pd.3988> PMID: 23097191
 27. Giles W, Bisits A, O'Callaghan S, Gill A (2003) The Doppler assessment in multiple pregnancy randomised controlled trial of ultrasound biometry versus umbilical artery Doppler ultrasound and biometry in twin pregnancy. *BJOG* 110: 593–597. PMID: 12798478
 28. Brosens I, Pijnenborg R, Benagiano G (2013) Defective myometrial spiral artery remodelling as a cause of major obstetrical syndromes in endometriosis and adenomyosis. *Placenta* 34: 100–105. <https://doi.org/10.1016/j.placenta.2012.11.017> PMID: 23232321
 29. Rizzo G, Arduini D, Romanini C (1992) Doppler echocardiographic assessment of fetal cardiac function. *Ultrasound Obstet Gynecol* 2: 434–445. <https://doi.org/10.1046/j.1469-0705.1992.02060434.x> PMID: 12796921
 30. Viscardi RM, Sun CC (2001) Placental lesion multiplicity: risk factor for IUGR and neonatal cranial ultrasound abnormalities. *Early Hum Dev* 62: 1–10. PMID: 11245990
 31. Muresan D, Rotar IC, Stamatian F (2016) The usefulness of fetal Doppler evaluation in early versus late onset intrauterine growth restriction. Review of the literature. *Med Ultrason* 18: 103–109. <https://doi.org/10.11152/mu.2013.2066.181.dop> PMID: 26962562
 32. Gaillard R, Arends LR, Steegers EA, Hofman A, Jaddoe VW (2013) Second- and third-trimester placental hemodynamics and the risks of pregnancy complications: the Generation R Study. *Am J Epidemiol* 177: 743–754. <https://doi.org/10.1093/aje/kws296> PMID: 23479346
 33. Mone F, Thompson A, Stewart MC, Ong S, Shields MD (2014) Fetal umbilical artery Doppler pulsatility index as a predictor of cardiovascular risk factors in children—a long-term follow up study. *J Matern Fetal Neonatal Med* 27: 1633–1636. <https://doi.org/10.3109/14767058.2013.871698> PMID: 24298956
 34. Lo JO, Roberts VHJ, Schabel MC, Wang X, Morgan TK, et al. (2018) Novel Detection of Placental Insufficiency by Magnetic Resonance Imaging in the Nonhuman Primate. *Reprod Sci* 25: 64–73. <https://doi.org/10.1177/1933719117699704> PMID: 28330415
 35. Crispi F, Hernandez-Andrade E, Pelsers MM, Plasencia W, Benavides-Serralde JA, et al. (2008) Cardiac dysfunction and cell damage across clinical stages of severity in growth-restricted fetuses. *Am J Obstet Gynecol* 199: 254 e251–258.
 36. Tei C, Ling LH, Hodge DO, Bailey KR, Oh JK, et al. (1995) New index of combined systolic and diastolic myocardial performance: a simple and reproducible measure of cardiac function—a study in normals and dilated cardiomyopathy. *J Cardiol* 26: 357–366. PMID: 8558414
 37. Bashiri A, Burstein E, Mazor M (2006) Cerebral palsy and fetal inflammatory response syndrome: a review. *J Perinat Med* 34: 5–12. <https://doi.org/10.1515/JPM.2006.001> PMID: 16489880
 38. Friedman D, Buyon J, Kim M, Glickstein JS (2003) Fetal cardiac function assessed by Doppler myocardial performance index (Tei Index). *Ultrasound Obstet Gynecol* 21: 33–36. <https://doi.org/10.1002/uog.11> PMID: 12528158
 39. Bahtiyar MO, Copel JA (2008) Cardiac changes in the intrauterine growth-restricted fetus. *Semin Perinatol* 32: 190–193. <https://doi.org/10.1053/j.semperi.2008.02.010> PMID: 18482620
 40. Ghawi H, Gendi S, Mallula K, Zghouzi M, Faza N, et al. (2013) Fetal left and right ventricle myocardial performance index: defining normal values for the second and third trimesters—single tertiary center experience. *Pediatr Cardiol* 34: 1808–1815. <https://doi.org/10.1007/s00246-013-0709-1> PMID: 23681419
 41. Nair A, Radhakrishnan S (2016) Fetal left ventricular myocardial performance index: Defining normal values for Indian population and a review of literature. *Ann Pediatr Cardiol* 9: 132–136. <https://doi.org/10.4103/0974-2069.177516> PMID: 27212847
 42. Letti Muller AL, Barrios Pde M, Kliemann LM, Valerio EG, Gasnier R, et al. (2010) Tei index to assess fetal cardiac performance in fetuses at risk for fetal inflammatory response syndrome. *Ultrasound Obstet Gynecol* 36: 26–31. <https://doi.org/10.1002/uog.7584> PMID: 20131338
 43. Romero R, Espinoza J, Goncalves LF, Gomez R, Medina L, et al. (2004) Fetal cardiac dysfunction in preterm premature rupture of membranes. *J Matern Fetal Neonatal Med* 16: 146–157. <https://doi.org/10.1080/14767050400009279> PMID: 15590440
 44. Wu D, Lei J, Rosenzweig JM, Burd I, Zhang J (2015) In utero localized diffusion MRI of the embryonic mouse brain microstructure and injury. *J Magn Reson Imaging* 42: 717–728. <https://doi.org/10.1002/jmri.24828> PMID: 25537944

45. Wu D, Lei J, Jia B, Xie H, Zhu Y, et al. (2018) In vivo assessment of the placental anatomy and perfusion in a mouse model of intrauterine inflammation. *J Magn Reson Imaging* 47: 1260–1267. <https://doi.org/10.1002/jmri.25867> PMID: 28981189
46. Andescavage N, duPlessis A, Metzler M, Bulas D, Vezina G, et al. (2017) In vivo assessment of placental and brain volumes in growth-restricted fetuses with and without fetal Doppler changes using quantitative 3D MRI. *J Perinatol* 37: 1278–1284. <https://doi.org/10.1038/jp.2017.129> PMID: 28837138